Hindawi
Mathematical Problems in Engineering
Volume 2018, Article ID 2394535, 11 pages
https://doi.org/10.1155/2018/2394535

Research Article

Speed Regulation of Permanent Magnet Synchronous Motor Using Event Triggered Sliding Mode Control

Huan Zhang, Qunying Liu, Jiashu Zhang, Shuheng Chen, and Changhua Zhang

School of Automation Engineering, University of Electronic Science and Technology, Chengdu, Sichuan 611731, China

Correspondence should be addressed to Qunying Liu; lqy1206@126.com

Received 10 July 2018; Revised 6 September 2018; Accepted 12 September 2018; Published 10 October 2018

Academic Editor: Xiangyu Meng

To reduce the chattering issue and improve the dynamic tracking performance of the speed regulation of the permanent magnet synchronous motor (PMSM) system, the sliding mode control (SMC) with an enhanced exponential reaching law (EERL) is proposed in this paper. Compared to the SMC with conventional reaching law (CRL), the proposed SMC based on the EERL makes the convergence rate be associated with the change of the system state variable. In order to implement the minimum resource utilization of the embedded processor while guaranteeing the performance of the system, the event triggered strategy is developed for SMC, which possesses the excellent robustness and saves the energy cost. The stability of the event triggered SMC control law is proved by the Lyapunov function and the minimum control execution time interval is also derived. Finally, the effectiveness of the proposed EERL and the satisfactory performance of the event triggered SMC are demonstrated by the simulation results.

1. Introduction

The PMSM is widely applied to industries due to its excellent characteristics, such as simple structure, small size, high power density, low noise, and friendly maintenance. However, the practical PMSM system is multivariable, strongly coupled, and nonlinear, which is easily affected by unmodeled dynamics, parameter variations, and load disturbance [1]. Therefore, the traditional linear control methods cannot effectively resolve these practical problems [2].

To decrease the influence of these aforementioned problems, various control theories have been proposed, such as fuzzy control [3], finite-time control [4], observer-based control [5], adaptive control [6], intelligent control [7, 8], and SMC [9–12]. The SMC has been widely applied to the PMSM system for its fast response, insensitive to parameter changes and disturbance, simple implementation, and strong robustness [9]. In [10], a sliding mode controller was designed for the SPMSM drive system, which was based on a novel error model with unknown load for the SPMSM drive system. To improve the performance the speed regulation of the PMSM, a robust fractional order sliding mode control has been proposed in [11]. The position controller of the PMSM was designed with an adaptive integral backstepping terminal SMC in [12], which can estimate the external disturbance and the moment of inertia. Also, an adaptive fuzzy SMC approach was proposed in [13], which aimed at the position regulation problem of the PMSM servo system. The SMC with a novel composite sliding mode control based on disturbance observer was applied to PMSM system [14].

However, the SMC is still troubled by the chattering phenomenon presently. The chattering phenomenon is that the output of the control signal is mixed with finite amplitude and high-frequency oscillation signal, which is damage to the mechanical system. In order to suppress the chattering issue, different approaches have been proposed, such as the integral sliding surface method [15], the observer-based method [16], and the reaching law approach [17, 18]. The reaching law method in [17] is an effective one as it can regulate the reaching process directly. The SMC based on the exponential reaching law was proposed in [18], which can accelerate the reaching time and suppress the chattering issue since the adoptive alteration of the coefficient of the sign function. In [19], power rate reaching law was proposed to reduce chattering. Although the different methods can reduce the chattering level to a certain extent, they generally have their limitations in application. Baek et al. [20] have proposed an adjustable reaching law by applying an

exponential term, which can reduce chattering and keep high tracking performance. Nevertheless, it cannot further improve the total harmonic distortion in power electronics applications.

Consequently, the EERL is proposed in this paper, which is based on the choice of an exponential term. In this method, the system state (error signal) is relative to the gain of the switching function. If the motion trajectories of the system state variables go far away from the sliding mode surface, the gain of the switching function will increase. On the contrary, if the motion trajectories of the system state variables are approaching the sliding mode surface, the gain of the sign function tends to zero. Hence, it can adapt to variations of the system state and sliding mode surface. Compared to the conventional SMC, the reaching law can reduce the reaching time and suppresses the chattering phenomenon.

In real work, the controllers are implemented on the digital platform. Therefore, the time triggered control scheme is commonly used, which is the periodic control method. In this strategy, the control law is updated at every sampling instants. Although this method is easy to implement, the source utilization is not economical. The event triggered strategy can avoid the unnecessary energy consumption under the premise of satisfactory control performances. The event triggered control loop is visualized in Figure 1, which includes two elements: an event triggering rule and a controller. The event triggered control loop is visualized in Figure 1 which includes two elements: an event triggering rule and a controller; the event triggering rule decides the sampling instant and updates the controller. In recent years, this method gains increasing attention and is investigated for many control problems. Tabuada and Paul [21] have investigated the event triggered real-time scheduling of stabilizing control tasks. It is different from the general approaches, which is applied to the real-time scheduling of the control task. This method can optimize schedules and reduce sampling rate. In [22], an event triggered control scheme has been studied for multiagent networked systems. In [23], a novel triggering condition for the directed communication links of the heterogenous multiagent systems was proposed and the observer was designed to estimate the internal state. The event triggered SMC of stochastic systems via output feedback [24] was studied, in which a state observer is designed to estimate the system state and to facilitate the design of sliding surface. The robust stability of linear time-invariant system based on event triggering strategy was discussed in [25]. The event triggered SMC was applied to the nonlinear system in [26], which is affected by the external disturbance. To solve the consensus problem for multiagent systems with output saturation, the distributed static and dynamic event triggered control law was proposed in [27]. Usually, the triggering event is decided by the discrete error [28], which is hard to realization and result the *Zeno phenomenon*. In [29], the periodic event triggered SMC was studied, whose result shows that there is no need to measure the continuous state. Nevertheless, it causes the instability of the system if the sampling period is chosen unsuitably. In [30], the event triggered SMC was applied to regulate the temperature of the continuous stirred tank reactor.

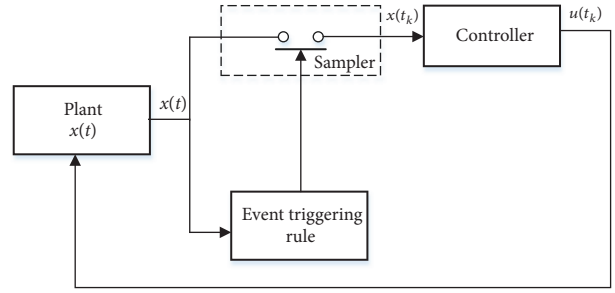

Figure 1: The event triggered control loop.

This paper is organized as follows. In Section 2, the dynamic model of the PMSM is introduced. The EERL is proposed and applied to the PMSM in Section 3. In Section 4, the event triggered SMC strategy is proposed and the stability of the system is analyzed. In Section 5 the simulation is carried out. The conclusions are drawn in Section 6.

2. The Dynamic Model of PMSM

Assuming that the distribution of the permanent magnetic field of the rotor is sinusoidal in the air gap space, induction electromotive force in armature winding is also sinusoidal. Considering that the saturation of stator core is neglected and magnetic circuit is linear, the inductance parameters are constant and the eddy current and hysteresis are overlooked. There is also no damping winding on the rotor. The mathematical model of surface mounted PMSM on $d-q$ coordinate is as follows:

$$\begin{aligned}
\frac{di_d}{dt} &= -\frac{R_s}{L_d} i_d + p_n w i_q + \frac{1}{L_d} u_d \\
\frac{di_q}{dt} &= -\frac{R_s}{L_d} i_q - p_n w i_d + \frac{1}{L_q} u_q - \frac{p_n w \phi_f}{L_q} \\
\frac{dw}{dt} &= -\frac{T_L}{J} + \frac{K_t}{J} i_q - \frac{Bw}{J}
\end{aligned} \tag{1}$$

where i_d and i_q are the currents of the stator d and q axes, respectively; u_d and u_q are the stator voltage of the d and q axes; R_s, L_d, and L_q are the stator resistance and the inductance of d and q axes, respectively; p_n is the number of pole pairs; K_t is the torque constant; J, B, T_L, and w are the system moment of inertia, viscous friction coefficient, load torque, and mechanical angular velocity, respectively. By defining a $= B/J$, $b = K_t/J$, $c = 1/J$, the motion equation of (1) can be rewritten as

$$\dot{w} = -aw + bi_q - \frac{1}{J} T_L \tag{2}$$

The state variables of the PMSM system is defined as

$$\begin{aligned}
x_1 &= w^* - w \\
x_2 &= \dot{w}^* - \dot{w}
\end{aligned} \tag{3}$$

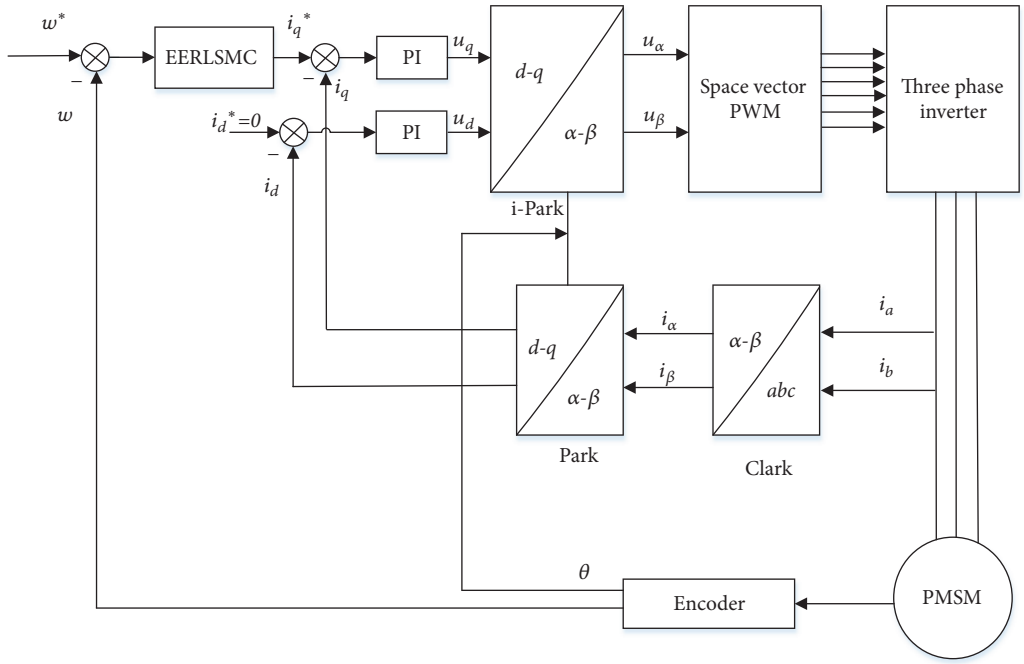

Figure 2: The control loop of PMSM.

where w^* is the reference speed. Assuming that there is a second derivative of w^*, (4) can be obtained according to (2) and (3):

$$\dot{x}_2 = \ddot{w}^* - \ddot{w} = \ddot{w}^* - \left(-a\dot{w} + b\dot{i}_q - c\dot{T}_L\right) \tag{4}$$

Equation (4) can be rewritten as

$$\begin{aligned}\dot{x}_2 &= -a\left(\dot{w}^* - \dot{w}\right) - b\dot{i}_q + c\dot{T}_L + a\dot{w}^* + \ddot{w}^* \\ &= -ax_2 - bu(t) + d(t)\end{aligned} \tag{5}$$

where $u(t) = \dot{i}_q$. The $d(t) = \ddot{w} + a\dot{w}^* + c\dot{T}_L$ represents the uncertainties of the system. The complete second-order dynamics model of the PMSM is

$$\begin{aligned}\dot{x}_1 &= x_2 \\ \dot{x}_2 &= -ax_2 - bu(t) + d(t)\end{aligned} \tag{6}$$

Actually, even though the parameters will change, the variable of the motor is bounded. Thus, $d(t)$ has an upper bound L_g, $|d(t)| \le L_g$, where L_g is a constant.

The vector form of (4) can be expressed as

$$\dot{x} = f(x) + B_1 u(t) + D(t) \tag{7}$$

where $f(x) = \begin{pmatrix} x_2 \\ -ax_2 \end{pmatrix}$, $B_1 = \begin{pmatrix} 0 \\ -b \end{pmatrix}$, and $D(t) = \begin{pmatrix} 0 \\ d(t) \end{pmatrix}$.

The vector control is adapted to the PMSM system in Figure 2, in which the PI algorithms are used to two current loops. In this paper, an enhanced reaching law sliding mode control method is proposed to improve the performance of the speed loop.

3. The Speed Controller Designed Based on Enhanced Exponential Reaching Law

In order to illustrate the proposed EERLSMC theory, the second-order nonlinear model is considered as

$$\begin{aligned}\dot{x}_1 &= x_2 \\ \dot{x}_2 &= A(x) + B(x)u(t) + G(x)\end{aligned} \tag{8}$$

where $x = \begin{pmatrix} x_1 \\ x_2 \end{pmatrix}$ is the state of the system; u is the control law; $A(x)$ and $B(x)$ are the bounded nonlinear function of the system state; $G(x)$ represents the matched disturbance. Assuming that $B(x) \neq 0$ and inevitable, the time varying sliding mode function is chosen as follows:

$$s(t) = c^T x \tag{9}$$

where $c^T = [c_1 \quad 1]$, c_1 is a strictly positive constant coefficient. The reaching condition of the sliding mode control is

$$s(t)\,\dot{s}(t) \le 0 \tag{10}$$

To satisfy expression (10), the reaching law is generally adopted as

$$\dot{s}(t) = -k \cdot \operatorname{sign}(s(t)) \tag{11}$$

where k is a positive constant coefficient and sign is the sign function.

Substituting (9) into (11), (12) is obtained as

$$c_1\dot{x}_1 + \dot{x}_2 = -k \cdot \operatorname{sign}(s(t)) \tag{12}$$

Then, substituting (8) into (12), the control law is written as

$$u(t) = -B^{-1}(x)\left(c_1 x_2 + A(x) + G(x) + k \cdot \operatorname{sign}(s(t))\right) \tag{13}$$

It is clear that the control law includes the discontinuous term. Increasing the coefficient k can cause the bigger chattering phenomenon. However, if the chattering value is up to k, several works have been done to suppress the chattering phenomenon by modifying reaching law. By integrating (11) between zero and t_{reach}, the reaching time can be obtained as

$$t_{reach} = \ln \frac{|s(0)|}{k} \tag{14}$$

The reaching time t_{reach} shows that, with k increasing, the reaching time becomes small while the chattering is increased. In [18], a constant rate reaching law is proposed as follows:

$$\dot{s}(t) = -q \cdot s(t) - k \cdot \operatorname{sign}(s(t)) \tag{15}$$

Integrating (15) with t, the reaching time can be presented by

$$t_{reach} = \frac{1}{k} \ln \frac{q|s(0)| + k}{k} \tag{16}$$

where q and k are positive constant coefficients; $s(0)$ is the initial value of the sliding mode function. Although constant reaching law can suppress the chattering phenomenon by increasing q and reducing k, the existence of the constant term of sign function cannot suppress the chattering well. The power rate reaching law in [19] is as follows:

$$s(t) = -k \cdot |s(t)|^{\beta} \operatorname{sign}(s(t)) \tag{17}$$

where k is the positive constant coefficient; β is the coefficient; and $\beta \in (0, 1)$.The reaching time is

$$t_{reach} = \frac{1}{(1-r)k} |s(0)|^{(1-\beta)} \tag{18}$$

The features of (17) are the robustness reduction, so the enhanced exponential reaching law is proposed to solve the above issues as follows:

$$\dot{s}(t) = -q \cdot s(t) - \frac{k}{E(s(t))} |s(t)|^{\beta} \operatorname{sign}(s(t)) \tag{19}$$

where $E(s(t)) = \delta + (1 + 1/|x_1| - \delta)e^{-\varsigma|s(t)|^r}$; k and q are the positive constant coefficients; δ and β are the coefficients with $\delta \in (0, 1)$ and $\beta \in (0, 1)$; ς and r are the positive integers.

It can be seen that $E(s(t))$ is positive at all time. Therefore, it has some influence on the SMC approach stability. From (19), it can be seen that when the system state $|x_1|$ raises, $E(s(t))$ goes towards the value of δ, and the gain of the sign function will approach $(k/\delta)|s(t)|^{\beta}$. On the contrary, if $|s(t)|$ decreases, $E(s(t))$ goes towards $(k/(1 + 1/|x_1|))|s(t)|^{\beta}$. Under this condition, the system state $|x_1|$ gradually tends to zero, which illustrates that when the system trajectory approaches the sliding mode surface, the coefficient of sign function will converge to zero to suppress the chattering. Therefore, it can dynamically adjust the reaching rate to the sliding surface according to the distance between the system state variables and the equilibrium point. Substituting the equation of (7) and (9) into (19), we can get the speed control law:

$$u(t) = b^{-1}\left(c^T f(x) + qs(t) + d(t) + \frac{k}{E(s)} |s(t)|^{\beta} \operatorname{sign}(s(t))\right) \tag{20}$$

In the speed control law (20), the disturbance $d(t)$ is unknown. To solve the question, $d(t)$ is replaced by its upper bound L_g. Then the following speed control law is designed as

$$u(t) = b^{-1}\left(c^T f(x) + qs(t) + \left(\frac{k}{E(s)} |s(t)|^{\beta} + L_g\right) \operatorname{sign}(s(t))\right) \tag{21}$$

According to the Lyapunov stability criterion, the Lyapunov function $V_1 = (1/2)s^2(t)$ is chosen. Substituting the equation of (7) and (21) into the time derivative of V_1, we get the following result:

$$\begin{aligned}
\dot{V}_1 &= s(t)\dot{s}(t) = s(t)\left(c_1 x_2 - a x_2 + d(t) - c^T f(x)\right. \\
&\quad \left. - qs(t) - \left(\frac{k}{E(s(t))} |s(t)|^{\beta} + L_g\right) \operatorname{sign}(s(t))\right) \\
&= s(t)\left(-qs(t)\right. \\
&\quad \left. - \left(\frac{k}{E(s(t))} |s(t)|^{\beta} + L_g\right) \operatorname{sign}(s(t)) + d(t)\right) \\
&= -qs^2(t) - \left(\frac{k}{E(s(t))} |s(t)|^{\beta} + L_g\right)|s(t)| + d(t) \\
&\quad \cdot s(t) = -qs(t)^2 - \frac{k}{E(s(t))} |s(t)|^{\beta+1} - \left(L_g |s(t)|\right. \\
&\quad \left. - d(t)s(t)\right) < -qs(t)^2 - \frac{k}{E(s(t))} |s(t)|^{\beta+1} < 0
\end{aligned} \tag{22}$$

Equation (22) ensures that the designed controller is asymptotically stable, and any tracking error equation (3) will be covered to zero in a finite time.

4. Event Triggered Sliding Mode Control

4.1. Stability Analysis. In practical implementation, the time triggered execution which also called Riemann sampling is generally adopted. The control law is only updated at a specific sampling instant via this method. Assuming the sampling instants $t = \{t_0, t_1, \ldots, t_k, \ldots\}$, $k \in N$ and the time interval $t_{k+1} - t_k$ is fixed constant, it is the periodic control.

In this paper, instead of relying on time triggered execution, the event triggered method is adopted, in which the control law is updated when the triggering rule is satisfied. Thus, the time interval $t_{k+1} - t_k \neq cons\tan t$; it is aperiodic control. Since the control law remains constant between two successive sampling instants, the control law applied to the system can express as

$$u(t_k) = b^{-1}\left(c^T f(x(t_k)) + qs(t_k) + \left(\frac{k}{E(s(t_k))}|s(t_k)|^{\beta} + L_g\right)\operatorname{sign}(s(t_k))\right) \tag{23}$$

where $t \in t_{k+1} - t_k$; $s(t_k) = c^T x(t_k)$.

Now the stability of the system is analyzed. It is defined that $S_1 \overset{def}{=\!=} \{x \in R^n : s = c^T x > 0\}$ and $S_2 \overset{def}{=\!=} \{x \in R^n : s = c^T x < 0\}$. Therefore, $R^n = S_1 \cup S_2 \cup S$ and at any time instant the trajectory remains in some one of the sets only. Then let us define

$$e(t) = x(t) - x(t_k) \quad \forall t \in [t_k, t_{k+1}) \tag{24}$$

where $x(t_k)$ is the value of system state of the triggering instant and $e(t)$ is the discrete error. It is induced in the system because the control law is discrete implementation and it plays a significant role in SMC. When the control law is updated at $t = t_k$ and at this time $e(t) = x(t) - x(t_k) = 0$, the trajectory reaches the sliding mode surface. For $t \in (t_k, t_{k+1})$, $e(t) \neq 0$, the trajectory is far away from the sliding mode surfacing.

Theorem 1. *Considering system (7) and control law (23), the actual sliding mode occurs in vicinity of the sliding manifold. If the manifold is attractive, the trajectories go towards it. In other words, it ensures the reachability to the surface, if the efficient* $L/q < \|x(t_k)\|/\|e(t)\|$ *is satisfied.*

L is the *Lipschitz constant* and q is the positive constant coefficient of the siding mode variable s.

Proof. Let the Lyapunov function $V_2 = (1/2)s^2(t)$, $t \in [t_k, t_{k+1})$. The time derivative of V_2 is

$$\dot{V}_2 = s(t)\,\dot{s}(t) = s(t)\left(c^T f(x) + B_1 u(t_k) + D(t)\right) \tag{25}$$

Substituting the control law (23) into (25), the following result can be obtained as

$$\begin{aligned}\dot{V}_2 &= s(t)\left(c^T f(x) + B_1 u(t_k) + D(t)\right)\\ &= s(t)\left(c^T f(x(t)) - c^T f(x(t_k)) - qs(t_k) - \left(\frac{k}{E(s(t_k))}|s(t_k)|^{\beta} + L_g\right)\operatorname{sign}(s(t_k)) + d(t)\right)\\ &= s(t)\left(c^T(f(x(t)) - f(x(t_k))\right) - s(t)\,qs(t_k) - s(t)\left(\frac{k}{E(s(t_k))}|s(t_k)|^{\beta} + L_g\right)\operatorname{sign}(s(t_k)) + s(t)\,d(t)\end{aligned} \tag{26}$$

Once $x \in S_1$ or $x \in S_2$, the $\operatorname{sign}(s(t)) = \operatorname{sign}(s(t_k))$, $\forall t \in [t_k, t_{k+1})$ is strictly met and $s(t) \neq 0$; $x(t) \neq 0$ is satisfied. Therefore, if the sliding manifold is not reached, (26) can be rewritten as

$$\begin{aligned}\dot{V}_2 &\leq \|s(t)\| \cdot \left\|c^T\right\| L \|x(t) - x(t_k)\| - \|s(t)\|\\ &\quad \cdot q\|s(t_k)\| - \|s(t)\| \cdot \left(\frac{k}{E(s(t_k))}\right)\|s(t_k)\|^{\beta}\\ &\quad - \left(L_g - d(t)\right)\|s(t)\|\\ &\leq -\|s(t)\| \cdot q\left\|c^T\right\| \cdot \|x(t_k)\| + \|s(t)\|\\ &\quad \cdot \left\|c^T\right\| L\|e(t)\|\\ &\leq -\|s(t)\| \cdot \left\|c^T\right\| (q\|x(t_k)\| - L\|e(t)\|)\end{aligned} \tag{27}$$

For $L/q < \|x(t_k)\|/\|e(t)\|$, (27) can be rewritten as

$$\begin{aligned}\dot{V}_2 &\leq -\|s(t)\| \cdot \left\|c^T\right\| (q\|x(t_k)\| - L\|e(t)\|)\\ &\leq -\varepsilon\|s(t)\|\end{aligned} \tag{28}$$

with $\varepsilon > 0$ in (28), it proves that the control strategy can drive the system trajectories asymptotically to the sliding mode surface in (9). When the control law is updated, $\|e(t)\| \longrightarrow 0$. Then (29) can be obtained.

$$\begin{aligned}\dot{V}_2 &\leq -\|s(t)\| \cdot \left\|c^T\right\| (q\|x(t_k)\| - L\|e(t)\|)\\ &\leq -\|s(t)\| \cdot \left\|c^T\right\| q\|x(t_k)\| < 0\end{aligned} \tag{29}$$

The asymptotic stability of system (7) is ensured by (29). The triggering rule is adopted in this paper which is proposed in [30] as follows:

$$\delta = \left\|\lambda_1 x_1 + \lambda_2 x_2^2\right\| - \lambda_3\left(m_1 + m_2 e^{-\lambda_4 t}\right) \tag{30}$$

where λ_1, λ_2, m_1, and m_2 are the positive constant coefficients; λ_3 and λ_4 are the coefficients and $\lambda_3, \lambda_4 \in (0, 1)$. In (30), $\lambda_3(m_1 + m_2 e^{-\lambda_4 t})$ guarantees a finite lower bound of the interval time between two triggering instants and avoids the *Zeno phenomenon* caused by accumulation of samples at same instant. The triggering rule decides the triggering instant. The next triggering instant is

$$t_{k+1} = \inf\left\{t \in \left(t_k, +\infty\right) : \delta > 0\right\}, \quad \forall k \in N \tag{31}$$

The interexecution time between two triggering instants is given by

$$T_k = t_{k+1} - t_k \tag{32}$$

□

4.2. The Given Minimum Bound for T_k

Theorem 2. *Considering system given by (7), control law (23), and error (24), when the triggering rule is satisfied, the triggering instants are $\{t_k\}_{k=0}^{\infty}$ and there is no Zeno phenomenon. Consequently, the interexecution time T_k has a lower bound which decides by a positive value and can be expressed as*

$$T_k \geq \frac{1}{L}\ln\left(\frac{L\|e\|_\infty}{L\left(1 + c^T L + qc^T + \left(k\left(c^T\right)^\beta/\delta\right)\|x(t_k)\|^{\beta-1} + 2L_g/L\right)\|x(t_k)\|} + 1\right) \tag{33}$$

where $\|e\|_\infty$ is the maximum discretization error.

Proof. The time derivate of (24) is

$$\begin{aligned}\frac{d}{dt}\|e(t)\| &\leq \left\|\frac{d}{dt}\overline{e}(t)\right\| \leq \left\|\frac{d}{dt}x(t)\right\| \\ &= \left\|f(x(t)) + B_1 u(t) + D(t)\right\|\end{aligned} \tag{34}$$

Substituting $x(t) = e(t) + x(t_k)$ into (23), (34) can be deduced as

$$\begin{aligned}\frac{d}{dt}\|e(t)\| &\leq \left\|f(x(t)) + D(t) + B_1 u(t_k)\right\| \\ &\leq \left\|f(x(t)) + D(t) - c^T f(x(t_k)) - qs(t_k)\right. \\ &\quad \left. - \left(\frac{k}{E(s(t_k))}|s(t_k)|^\beta + L_g\right)\operatorname{sign}(s(t_k))\right\| \\ &\leq L\|x(t)\| + c^T L\|x(t_k)\| + qc^T\|x(t_k)\| + L_g \\ &\quad + \frac{k\left(c^T\right)^\beta}{\delta}\|x(t_k)\|^\beta + L_g \leq L\left(\|e(t)\| + \|x(t_k)\|\right) \\ &\quad + c^T L\|x(t_k)\| + qc^T\|x(t_k)\| + \frac{k\left(c^T\right)^\beta}{\delta}\|x(t_k)\|^\beta \\ &\quad + 2L_g \leq L\left(\|e(t)\|\right) + L\left(1 + c^T L + qc^T\right. \\ &\quad \left. + \frac{k\left(c^T\right)^\beta}{\delta}\|x(t_k)\|^{\beta-1} + \frac{2L_g}{L}\right)\|x(t_k)\|\end{aligned} \tag{35}$$

with the initial condition $e(t_k) = x(t) - x(t_k) = 0$, the solution to (35) is obtained by invoking the comparison lemma [31] as follows:

$$\|e(t)\| \leq \frac{L\left(1 + c^T L + qc^T + \left(k\left(c^T\right)^\beta/\delta\right)\|x(t_k)\|^{\beta-1} + 2L_g/L\right)\|x(t_k)\|}{L}\left\{\exp\left(L\left(t - t_k\right)\right) - 1\right\} \tag{36}$$

Then

$$\|e\|_\infty = \|e(t_{k+1})\| \leq \frac{L\left(1 + c^T L + qc^T + \left(k\left(c^T\right)^\beta/\delta\right)\|x(t_k)\|^{\beta-1} + 2L_g/L\right)\|x(t_k)\|}{L}\left(e^{LT_k} - 1\right) \tag{37}$$

So the interexecution time T_k can be expressed as

$$T_k \geq \frac{1}{L}\ln\left(\frac{L\|e\|_\infty}{L\left(1 + c^T L + qc^T + \left(k\left(c^T\right)^\beta/\delta\right)\|x(t_k)\|^{\beta-1} + 2L_g/L\right)\|x(t_k)\|} + 1\right) \tag{38}$$

Table 1: Parameters of PMSM.

Characteristic	Symbol	Value
Stator phase resistance	R	2.875 Ω
d- and q-axes inductances	$L_d = L_q$	8.5 mH
Number of pole pairs	p_n	4
viscous damping	B	0.008 N. m. s
Torque Constant	K_t	1.05 N. m
Rotational inertia	J	0.003 kg.m2

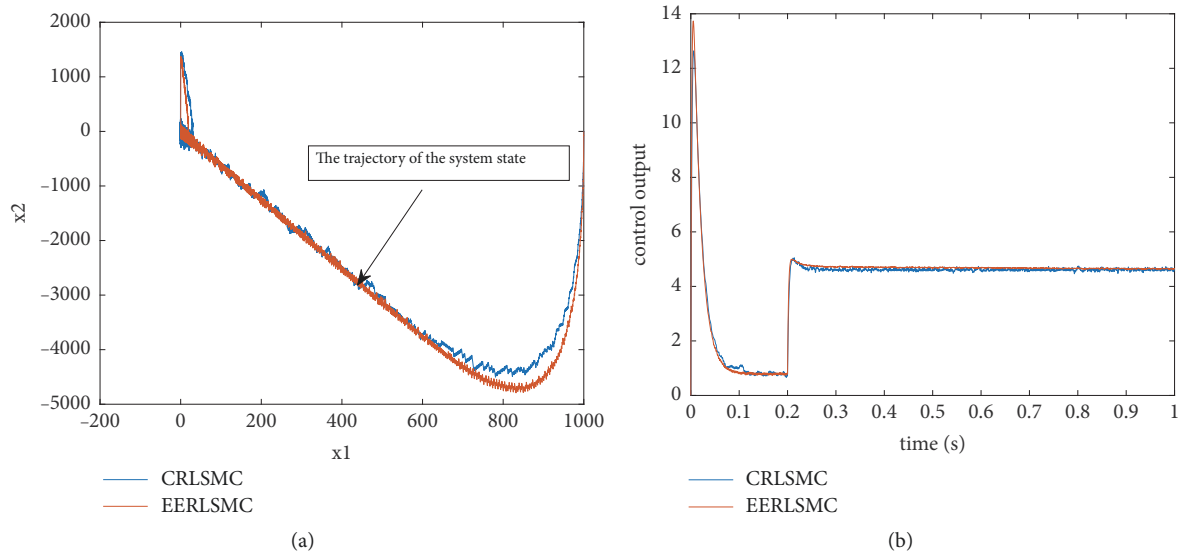

Figure 3: Comparison of the trajectory of system state and the controller output of the two methods. (a) The trajectory of sliding mode control of the two methods. (b) The controller output of the two methods.

Theorem 2 is proved by (16). It can conclude that the interevent execution time is bounded below a finite positive quantity. □

5. Results and Discussion

5.1. Simulation Results of the Dynamic Speed Response. In this paper, the vector control $i_d^* = 0$ is adopted, according to the control structure in Figure 2. The specific implementation steps include the following: Step (1): the simulation model of permanent magnet synchronous motor speed regulation system is established in Matlab/Simulink, which is a double closed loop system. Step (2): the EERLSMC and CRLSMC are applied to the speed control loop to verify the effectiveness of the proposed reaching law. Step (3): the parameters of PMSM and initial conditions are set as shown in Table 1.

In the simulation, the disturbances are not considered. So let L_g=0; the simulation conditions are as follows: the DC voltage of the inverter is 311 V; the switching frequency of the PWM $f = 10\ kHz$; the simulation step $T_s = 1e - 5$ s; the simulation time $t = 0.4$. The reference speed $w^* = 1000$ RPM; the initial load $T_L = 0$ N.m; the load 4 N.m is added at 0.2 s and not removed. The speed loop parameters of the CRLSMC are $k = 200$ and $q = 300$. The parameters of EERLSMC are $k = 200$, $q = 300$, $r = 2$, $\varsigma = 10$, $\beta = 0.8$, and $\delta = 0.5$. Above all, the simulation results are shown as Figures 3–5.

Figure 3(a) shows the comparison of the trajectories of system states of the two methods, from which it indicates that the vicinity of the proposed method is smaller than the CRL. Figure 3(b) shows the difference between the two methods in the control output, which illustrates that the control output curve of the EERLSMC is smoother.

Figures 4(a) and 4(b) demonstrate the improved performance of the two controllers. Figure 4(a) shows that when the speed increases from 0 to 1000 RPM, the proposed method only needs 0.15 s to reach the stable state, while the CRLSMC still has a slight oscillation. When the system reaches the desired speed, the controller based on EERLSMC has a smaller chattering phenomenon. Moreover, when the load torque $T_L = 0$ N.M is added to $T_L = 4$ N.m at t = 0.2 s, both methods are affected by sudden increase of the load. During this process, the chattering phenomenon and speed deviation are accompanied. At about 0.2 s, the speed of EERLSMC is 980, that of the CRL is only 970, and the EERLSMC only needs smaller time to the desired speed. Obviously, EERLSMC method gives less speed fluctuation and electrical magnetic torque fluctuations is smaller and smoother. Of course, it has a better robustness. The EERLSMC torque in

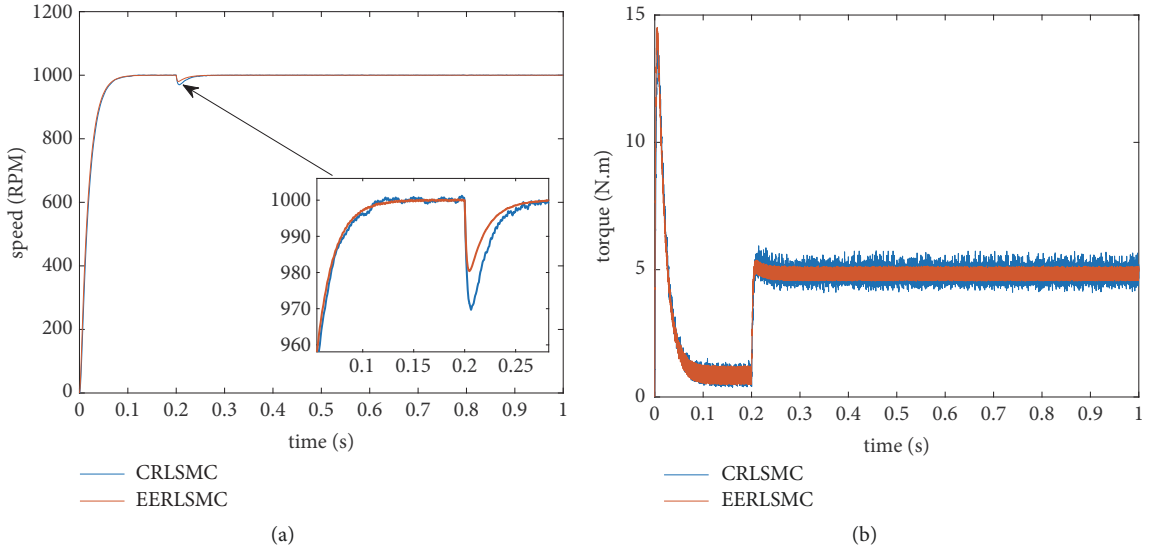

Figure 4: Comparison of the speed/torque response of the two methods. (a) Speed curve of the two methods. (b) Torque curve of the two methods.

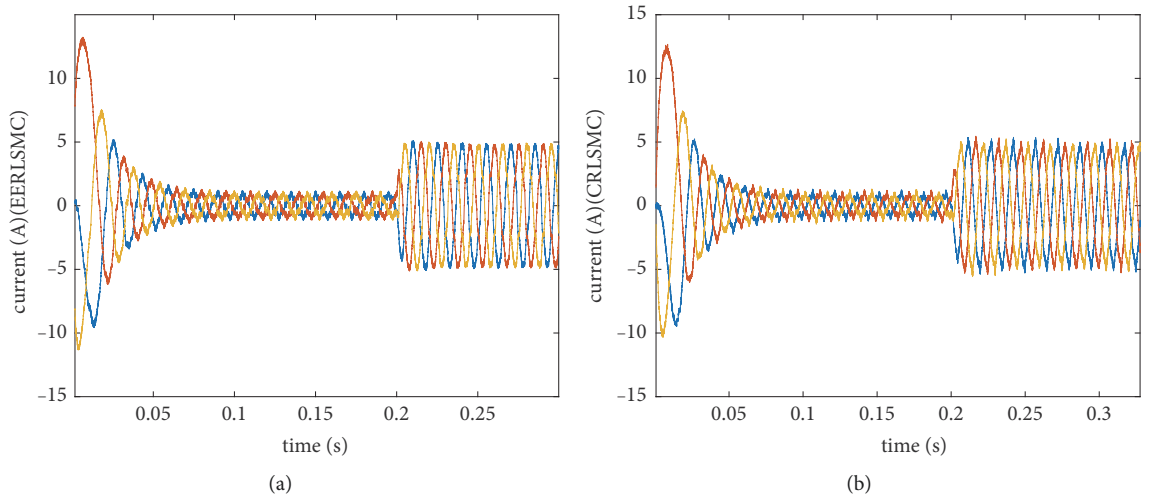

Figure 5: Comparison of current response of the two methods. (a) The three-phase stator current based on EERLSMC method. (b) The three-phase stator current based on CRLSMC method.

Figure 4(b) shows lower harmonic magnitudes compared with the torque associated with the CRL.

Figure 5 shows the three-phase stator current curves of PMSM under the two methods. Compared with the CRLSMC, the curve controlled by EERLSMC is smoother.

5.2. Simulation Results of the Event Triggered EERLSMC. Section 5.1 illustrates the good performance of the EERLSMC to the speed regulation of the PMSM system, then, this part the event triggered strategy is added to the EERLSMC. The parameters of the triggering rule are $\lambda_1 = 0.9$, $\lambda_2 = 9.9e - 6$, $\lambda_3 = 0.8$, $\lambda_4 = 0.9$ $m_1 = 1e - 5$, and $m_2 = 0.13$. Based on MATLAB/Simulink, the effectiveness of the proposed event triggered EESMC is demonstrated by Figures 6(a)–6(d) and Figure 7.

Figure 6 demonstrates the performances of the event triggered EERLSMC. Figure 6(a) shows the speed regulation results, in which it shows that the performance of the PMSM system can be satisfied as Figure 4(a). This proves that even though the choice of the sampling time is based on the event triggered rule, the performance is still satisfactory. However, if the control task executes as rarely as possible, the processor will have more time to complete other important tasks. Figures 6(b)–6(d) give the plots of the system states and sliding trajectory. The system trajectory is attracted towards to the sliding manifold s and the trajectories are ultimately bounded in steady and hence the system is stable. Figure 7 gives the triggering instant t_k. The vertical axis is the simulation time and the horizontal axis is the triggering instant t_k; we can see that, at first the system has not reached

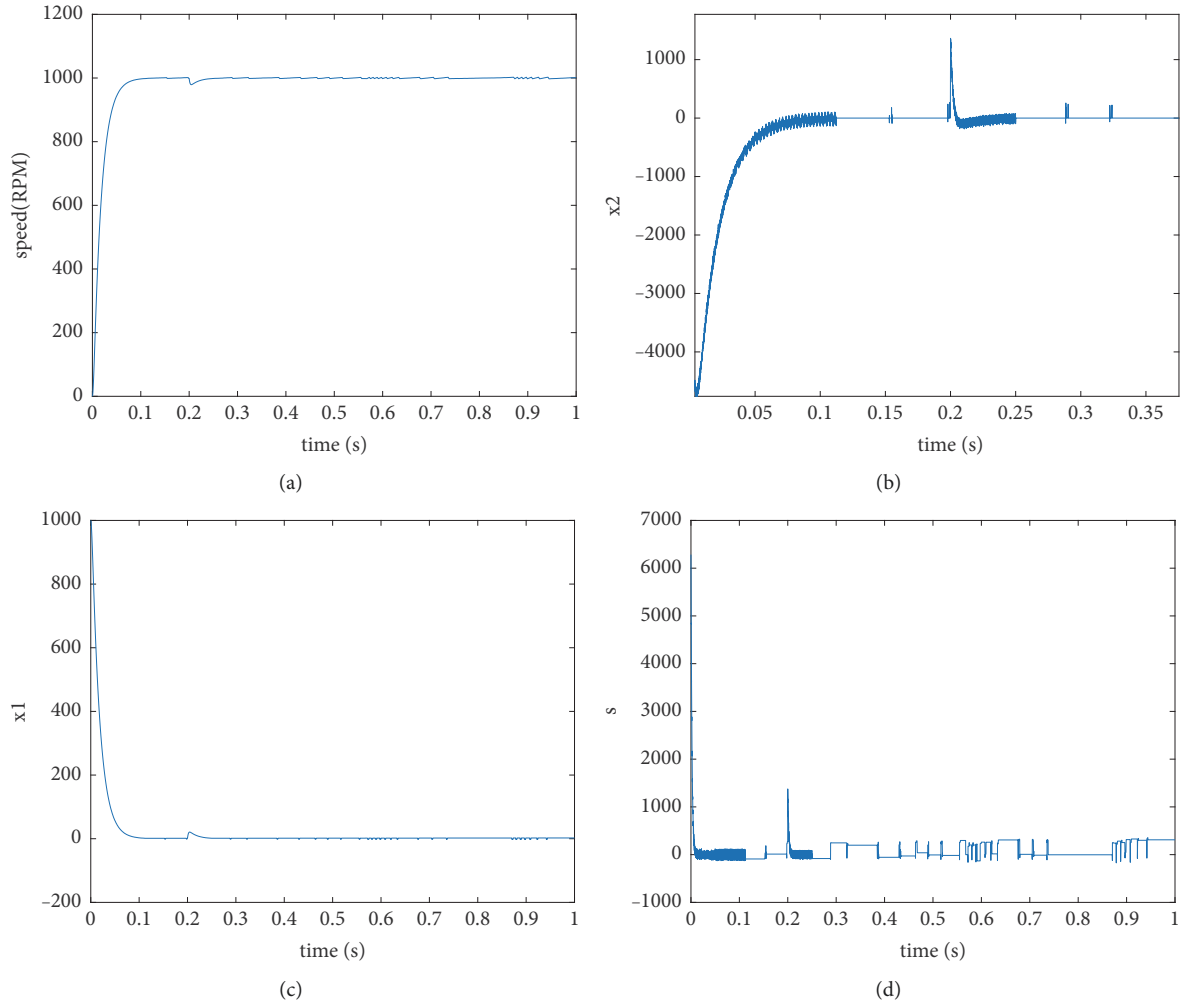

Figure 6: (a) Speed regulation at 1000 RPM. (b) System state variable x_1. (c) System state variable x_2. (d) Sliding surface s.

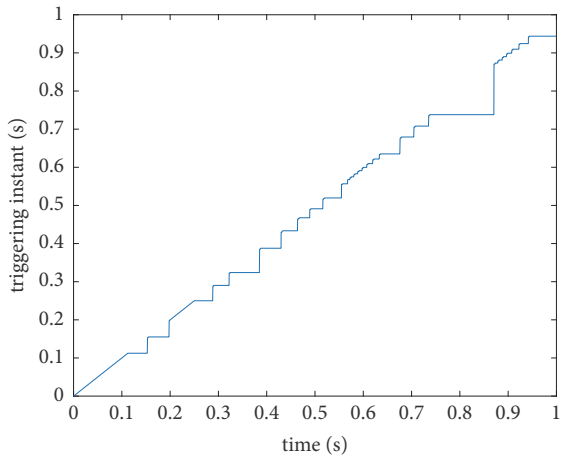

Figure 7: The triggering instants t_k.

the steady state, the time interval is close to the simulation step size; however, it will become bigger than simulation step size when the system is stable. Obviously, the sampling instant is not periodic and the controller is updated only at specific instant based on the triggering rule, by which the calculation cost is reduced and the energy is saved.

6. Conclusions

In this paper, an enhanced reaching law based on the exponential term is proposed and the stability of the EERLSMC has proved by the Lyapunov function. The proposed reaching law is applied to the speed regulation of the PMSM system. Then, the event triggered SMC is devised for the PMSM control system, by which the control law is updated when the triggering rule is satisfied. From the simulations and the comparisons, the following conclusions can be drawn: (1) The proposed reaching law can effectively suppress the chattering phenomenon and improve the reaching time and make the motor system more stable. (2) Compared to the SMC with conventional reaching law, the proposed SMC based on the EERL makes the convergence rate is associated with the change of the system state variable, which has a fast calculation. (3) Through the simulations, the effectiveness

of the proposed event triggered SMC has been verified. The stability of the system is guaranteed. The interval time between two triggering instants is greater than the time triggered. Due to the bigger sampling interval, the controller executes as little as possible. Thus, the energy consumption which is owing to the communication is minimized. Even if the energy is not a concern, the control tasks are executed infrequently, so that the processor will have more time to complete other important tasks.

Data Availability

The data used to support the findings of this study are available from the corresponding author upon request.

Conflicts of Interest

The authors declare that there are no conflicts of interest regarding the publication of this paper.

Acknowledgments

The work described in this paper was supported in part by Natural Science Foundation of China under Grant NSFC51677020, in part by the Provincial Key Laboratory of Power Electronics Energy Saving Technology and Equipment (no. szjj2016-093), in part by China Postdoctoral Science Foundation under Grant 2015M572457, and in part by Fundamental Research Funds for the Central Universities (no. ZYGX2016J209).

References

[1] K.-H. Kim and M.-J. Youn, "A nonlinear speed control for a PM synchronous motor using a simple disturbance estimation technique," *IEEE Transactions on Industrial Electronics*, vol. 49, no. 3, pp. 524–535, 2002.

[2] M. Tursini, F. Parasiliti, and D. Zhang, "Real-time gain tuning of PI controllers for high-performance PMSM drives," *IEEE Transactions on Industry Applications*, vol. 38, no. 4, pp. 1018–1026, 2002.

[3] A. V. Sant, "PM synchronous motor speed control using hybrid fuzzy-PI with novel switching functions," *IEEE Transactions on Magnetics*, vol. 45, no. 10, pp. 4672–4675, 2009.

[4] M. Preindl and S. Bolognani, "Model predictive direct speed control with finite control set of PMSM drive systems," *IEEE Transactions on Power Electronics*, vol. 28, no. 2, pp. 1007–1015, 2013.

[5] Q. Ling, J. Li, and H. Deng, "Robust Speed Tracking of Networked PMSM Servo Systems with Uncertain Feedback Delay and Load Torque Disturbance," *Journal of Applied Mathematics*, vol. 2012, Article ID 365923, 17 pages, 2012.

[6] Y. A.-R. I. Mohamed, "Adaptive self-tuning speed control for permanent-magnet synchronous motor drive with dead time," *IEEE Transactions on Energy Conversion*, vol. 21, no. 4, pp. 855–862, 2006.

[7] F.-J. Lin and P.-H. Shen, "Adaptive fuzzy-neural-network control for a DSP-based permanent magnet linear synchronous motor servo drive," *IEEE Transactions on Fuzzy Systems*, vol. 14, no. 4, pp. 481–495, 2006.

[8] F. M. Fayez, "Intelligent optimal recurrent wavelet elman neural network control system for permanent-magnet synchronous motor servo drive," *IEEE Transactions on Industrial Informatics*, vol. 9, no. 4, pp. 1986–2003, 2013.

[9] S. Li, M. Zhou, and X. Yu, "Design and implementation of terminal sliding mode control method for PMSM speed regulation system," *IEEE Transactions on Industrial Electronics*, vol. 9, no. 4, pp. 1879–1891, 2013.

[10] B.-J. Wang and J.-J. Wang, "Sliding mode control of surface-mount permanent-magnet synchronous motor based on error model with unknown load," *Journal of Software* , vol. 6, no. 5, pp. 819–825, 2011.

[11] J. Huang, H. Li, Y. Q. Chen, and Q. Xu, "Robust Position Control of PMSM Using Fractional-Order Sliding Mode Controller," *Abstract Applied Analysis*, vol. 4, pp. 473–505, 2012.

[12] H. Shi, Y. Feng, and X. Yu, "Adaptive backstepping hybrid terminal sliding-mode control for permanent magnet synchronous motor," in *Proceedings of the 2010 11th International Workshop on Variable Structure Systems, VSS 2010*, pp. 272–276, Mexico, June 2010.

[13] Y. Wang and J. Fei, "Adaptive fuzzy sliding mode control for PMSM position regulation system," *International Journal of Innovative Computing Information & Control Ijicic*, vol. 11, no. 3, pp. 881–891, 2015.

[14] J. Huang, L. Cui, X. Shi, H. Li, and Z. Xiang, "Composite integral sliding mode control for PMSM," in *Proceedings of the 33rd Chinese Control Conference, CCC 2014*, pp. 8086–8090, China, July 2014.

[15] C. Xia, X. Wang, S. Li, and X. Chen, "Improved integral sliding mode control methods for speed control of pmsm system," *International Journal of Innovative Computing Information & Control Ijicic*, vol. 7, no. 4, pp. 1971–1982, 2011.

[16] O. Barambones and P. Alkorta, "Position control of the induction motor using an adaptive sliding-mode controller and observers," *IEEE Transactions on Industrial Electronics*, vol. 61, no. 12, pp. 6556–6565, 2014.

[17] Y. Liu, B. Zhou, H. Wang, and S. Fang, "A new sliding mode control for Permanent Magnet Synchronous Motor drive system based on reaching law control," in *4th IEEE Conference on Industrial Electronics and Applications*, pp. 1046–1050, Xi'an, 2009.

[18] C. J. Fallaha, M. Saad, H. Y. Kanaan, and K. Al-Haddad, "Sliding-mode robot control with exponential reaching law," *IEEE Transactions on Industrial Electronics*, vol. 58, no. 2, pp. 600–610, 2011.

[19] S. Navaneethan and J. Jerome, "Speed control of permanent magnet synchronous motor using power reaching law based sliding mode controller," *WSEAS Transactions on Systems and Control*, vol. 10, pp. 270–277, 2015.

[20] J. Baek, M. Jin, and S. Han, "A new adaptive sliding-mode control scheme for application to robot manipulators," *IEEE Transactions on Industrial Electronics*, vol. 63, no. 6, pp. 3628–3637, 2016.

[21] P. Tabuada, "Event-triggered real-time scheduling of stabilizing control tasks," *IEEE Transactions on Automatic Control*, vol. 52, no. 9, pp. 1680–1685, 2007.

[22] X. Meng and T. Chen, "Event based agreement protocols for multi-agent networks," *Automatica*, vol. 49, no. 7, pp. 2125–2132, 2013.

[23] X. Meng, L. Xie, and Y. C. Soh, "Event-Triggered Output Regulation of Heterogeneous Multi-Agent Networks," *IEEE Transactions on Automatic Control*, 2018.

[24] L. Wu, Y. Gao, J. Liu, and H. Li, "Event-triggered sliding mode control of stochastic systems via output feedback," *Automatica*, vol. 82, pp. 79–92, 2017.

[25] A. K. Behera and B. Bandyopadhyay, "Event based robust stabilization of linear systems," in *Proceedings of the IECON 2014 - 40th Annual Conference of the IEEE Industrial Electronics Society*, pp. 133–138, Dallas, TX, USA, October 2014.

[26] J. Zhang, C. Peng, D. Du, and M. Zheng, "Adaptive event-triggered communication scheme for networked control systems with randomly occurring nonlinearities and uncertainties," *Neurocomputing*, vol. 174, pp. 475–482, 2016.

[27] X. Yi, T. Yang, J. Wu, and K. H. Johansson, "Event-triggered control for multi-agent systems with output saturation," in *Proceedings of the 2017 36th Chinese Control Conference (CCC)*, pp. 8431–8436, Dalian, China, July 2017.

[28] A. K. Behera and B. Bandyopadhyay, "Event-triggered sliding mode control for a class of nonlinear systems," *International Journal of Control*, vol. 89, no. 9, pp. 1916–1931, 2016.

[29] A. K. Behera, B. Bandyopadhyay, and X. Yu, "Periodic event-triggered sliding mode control," *Automatica*, vol. 96, pp. 61–72, 2018.

[30] A. Sinha and R. K. Mishra, "Control of a nonlinear continuous stirred tank reactor via event triggered sliding modes," *Chemical Engineering Science*, vol. 187, pp. 52–59, 2018.

[31] H. K. Khalil, *Nonlinear Systems*, Prentice-Hall, Inc, Upper Saddle River, NJ, USA, 3rd edition, 2002.